

UC Davis

UC Davis Previously Published Works

Title

Myelin injury and degraded myelin vesicles in Alzheimer's disease.

Permalink

<https://escholarship.org/uc/item/6h41t219>

Journal

Current Alzheimer Research, 11(3)

ISSN

1567-2050

Authors

Zhan, Xinhua

Jickling, Glen C

Ander, Bradley P

et al.

Publication Date

2014-03-01

DOI

10.2174/1567205011666140131120922

Peer reviewed

Published in final edited form as:

*Curr Alzheimer Res.* 2014 March ; 11(3): 232–238.

## Myelin injury and degraded myelin vesicles in Alzheimer's disease

X Zhan<sup>1</sup>, GC Jickling<sup>1</sup>, BP Ander<sup>1</sup>, D Liu, B Stamova<sup>1</sup>, C Cox<sup>1</sup>, LW Jin<sup>2,3</sup>, C DeCarli<sup>1,2</sup>, and FR Sharp<sup>1</sup>

<sup>1</sup>Department of Neurology, MIND Institute, University of California at Davis, Sacramento, CA

<sup>2</sup>Alzheimer's Disease Center, University of California at Davis, Sacramento, CA

<sup>3</sup>Department of Pathology, University of California at Davis, Sacramento, CA

### Abstract

**Objective**—Myelin disruption is an important feature of Alzheimer's disease (AD) that contributes to impairment of neuronal circuitry and cognition. In this study we characterize myelin degradation in the brains of patients with Alzheimer's disease compared with normal aged controls.

**Methods**—Myelin from patients with AD (n=13) was compared to matched controls (n=6). Myelin degradation was examined by immunohistochemistry in frontal white matter (WM) for intact myelin basic protein (MBP), degraded MBP, the presence of myelin lipid and for PAS staining. The relationship of myelin degradation and axonal injury was also assessed.

**Results**—Brains from patients with AD had significant loss of intact MBP, and an increase in degraded MBP in periventricular WM adjacent to a denuded ependymal layer. In regions of myelin degradation, vesicles were identified that stained positive for degraded MBP, myelin lipid, and neurofilament but not for intact MBP. Most vesicles stained for PAS, a corpora amylacea marker. The vesicles were significantly more abundant in the periventricular WM of AD patients compared to controls (44.5±11.0 versus 1.7±1.1,  $p=0.02$ ).

**Conclusion**—In AD patients degraded MBP is associated in part with vesicles particularly in periventricular WM that is adjacent to areas of ependymal injury.

### Keywords

myelin basic protein; myelin degradation; ependyma; corpora amylacea; Alzheimer's

### Introduction

Disruption of myelin contributes to cognitive impairment in Alzheimer's disease (AD) [1–8]. Improved understanding of myelin damage in AD may identify novel targets to reduce its

---

Correspondence to Xinhua Zhan, M.D., Ph.D., University of California at Davis, M.I.N.D. Institute Room 2415, 2805 50<sup>th</sup> Street, Sacramento, CA 95817, USA Telephone: 916-703-0449. FAX: 916-703-0369. xzhan@ucdavis.edu.

#### Conflict of interest

The authors declare no conflict of interest.

degradation and thus slow cognitive decline. In this study we sought to evaluate the molecular characteristics of myelin degradation in AD.

The presence of myelin disruption and intracellular lipid deposits in AD was initially described by Alois Alzheimer in 1911 [9, 10]. The roles of these lipid deposits and disrupted myelin have received some study [11, 12] including a description of decreased myelin lipids in brain [1] and increased levels of ceramide in the CSF [13], and brain parenchyma [6, 14]. Furthermore, neuroimaging studies have shown a greater loss of myelin integrity in patients with AD compared to controls [15] and that the loss of myelin integrity precedes the onset of cognitive impairment [2]. These findings support the notion that myelin degradation is an important component of AD.

Based on these evolving concepts, we sought to further evaluate myelin degradation in AD, and determine the fate of degraded myelin. We selected frontal lobe white matter since this region is commonly involved in AD patients [2]. We demonstrate that AD patients have a reduction in intact myelin basic protein (MBP) compared to controls. In these regions of reduced myelin, patients with AD have increased number of vesicles containing degraded myelin, myelin lipids and axonal proteins compared to control brain. Most vesicles also stain for PAS, a corpora amylacea marker. Furthermore, degradation of myelin is shown to be associated with disruption to ependymal cells adjacent to the periventricular white matter (PVWM) which we postulate may promote myelin damage and thus warrant further study.

## Material and Methods

### Brain Samples

AD and control brains were provided by the Alzheimer's Disease Center at University of California Davis. The study was approved by the Institutional Review Board. Informed consent to share research tissue after death was obtained from all patients or a representative prior to their death. The clinical diagnosis of AD was made by board certified neurologists and pathological diagnosis confirmed by board certified neuropathologists. AD was rated by CERAD criteria and staging of Braak [16]. A total of 19 brains including 13 AD and 6 controls were studied. Controls were normal individuals with low likelihood of clinical AD or Lewy body dementia and who did not meet criteria for AD neuropathology. They were matched to AD based on age and gender.

Brains were fixed in formalin. Blocks of tissue including frontal periventricular white matter (PVWM) and deep white matter (DWM) at the level of the head of the caudate nucleus from each brain were removed and embedded in paraffin. Sections were cut in the coronal plane.

### Immunohistochemistry

Paraffin was removed with xylene (5 minutes x 3 times) followed by ethanol (5 min in 100%, 5 min in 95% and 5 min in 70%). Antigen retrieval was performed in 25mM Tris, 3mM KCL, 140mM NaCl, 1mM EDTA and 0.05% Tween 20 in distilled water at 95°C for 20 min. Brain sections were then treated with 3% H<sub>2</sub>O<sub>2</sub> in PBS for 20 minutes to quench endogenous peroxidase activity. Nonspecific binding was blocked with 2% goat serum, 1% BSA and 0.3% Triton 100 in 0.1 M PBS. Sections were then incubated with primary

antibodies overnight at 4°C. The secondary antibody was a biotinylated goat anti-mouse or goat anti-rabbit IgG (1:200 dilution, Vector Labs, USA) depending on the species of the primary antibodies. The secondary antibody was incubated for 60 minutes at room temperature and then rinsed with PBS. The antibody complex was detected using ABC reagent and a substrate solution of H<sub>2</sub>O<sub>2</sub> and diaminobenzidine according to the manufacturer's instructions (Vector Labs). The primary antibody was omitted to assess non-specific staining.

### Immunofluorescence

After eliminating autofluorescence using the Autofluorescence Eliminator Reagent (Millipore, USA) and blocking nonspecific sites, sections were incubated with primary antibody. Goat anti-mouse or goat anti-rabbit Alexa Fluor® 488 or 594 conjugated antibodies (Invitrogen, USA) were used for secondary antibodies depending on the species of the primary antibody.

The primary antibodies used in the study were diluted at 1:500 unless otherwise stated. The antibodies included mouse monoclonals against myelin basic protein (MBP) (Millipore, 1:500 dilution), neurofilament protein (NF) (Pan-axonal Neurofilament Marker, Covance, 1:1000 dilution), and the myelin lipid galactocerebroside (GALC) (Millipore). In addition, rabbit polyclonals were used against degraded myelin basic protein (dMBP) (Millipore) and the neurofilament light chain (NF-L, Millipore, 1:1000 dilution).

### Staining for PAS and dMBP

To stain sections for the corpora amylacea (CA) marker PAS, sections were incubated in 0.5% periodic acid (Sigma) for 5 min at room temperature followed by washing in tap water for 1 minute. Then sections were incubated in Schiff reagent (Sigma) for 10 min followed by washing in tap water for 10 min. Then, after rinsing in PBS for 10 minutes and blocking nonspecific sites, sections were immunostained for dMBP using the antibody and procedures outlined above. Regular aqueous mounting medium was used to apply cover slips after the staining since the anti-fade mounting medium for fluorescence bleached the PAS staining. Sections were photographed under bright field for PAS staining and under fluorescence for dMBP staining.

### Quantitative Analysis

Sections including frontal PVWM and DWM at the level of the head of the caudate nucleus from each brain were used for counting dMBP<sup>+</sup> vesicles and evaluating ependymal damage. Three sections per brain were counted. Sections from all cases including 13 AD subjects and 6 control subjects were analyzed. Only clearly stained, round to oval vesicles were counted. PVWM was defined as the WM within 10.0 mm of the ependymal cell layer. PVSR was defined as the WM region within 1.0 mm from the endothelial cells of the vessels. The numbers of vesicles were counted in random 20X field area (about 0.8 mm<sup>2</sup>) in DWM, perivascular regions (PVSR) and PVWM in each of the sections by a blinded investigator. For each of the AD and control brains the degree of ependymal loss along the ventricular wall on each section was graded according to the following scale: "mild" with ependyma

loss 25%; “moderate” with ependyma loss >25% and 50%; and “severe” with ependyma loss > 50%.

### Statistical Analysis

Differences between groups were analyzed using a Student’s t-test (continuous), Wilcoxon-Mann Whitney test (ordinal) or Fisher Exact test (categorical). A P value 0.05 was considered significant.

### Results

Postmortem brain tissue samples were obtained from 13 patients with AD and 6 control subjects (Table 1). The average age of the control and AD subjects was  $79.8 \pm 3.2$  and  $83.7 \pm 1.5$  (Mean  $\pm$  SE) years old, respectively. There were no significant differences in age and gender among AD and controls. The median for the Braak stage was 6 in AD patients, and was 2 in cognitively normal controls ( $P < 0.001$ ).

### Myelin Degradation in AD Brains

In controls, intense MBP staining was seen in the periventricular white matter (PVWM) (Fig. 1A1) and white matter regions adjacent to perivascular regions (PVSR) in deep white matter (DWM) (Fig. 1A2). In PVWM of AD brains there was patchy loss of ependymal cells (Fig. 1B1, right side of solid black line). There was a decrease of intact-MBP staining adjacent to areas where the ependyma was denuded (Fig. 1B1, red arrow). MBP staining was less affected in areas where ependyma was intact (Fig. 1B1, left of solid black line). Decreased intact MBP staining also occurred in PVSR in DWM of AD brains (Fig. 1B2). Vesicles (which were MBP negative) were observed in areas of myelin loss in the perivascular regions (PVSR) in AD brains (Fig. 1B2, arrows). There was significantly more ependymal damage in AD compared to control brains with 11 of 13 AD brains showing severe ependymal damage whereas only 1 of 6 control brains showed severe ependymal damage ( $P=0.009$ ) (Table 1).

### Identification of Degraded Myelin Vesicles in Aged and AD brains

Since staining of intact MBP was decreased and vesicles (which did not stain for MBP) were observed in WM of the AD brains, we used a specific antibody against degraded MBP (dMBP) to determine where the degraded myelin might accumulate. This antibody detected numerous vesicles in the PVWM (Fig. 1D1, arrows) and PVSR (Fig. 1D2, arrows) of AD brains. These dMBP<sup>+</sup> vesicles can be categorized based on their different immunoreactive patterns: solid vesicles (Figs. 1D1 and 1D2, white arrows), clear vesicles (Figs. 1D1 and 1D2, black arrows) and those with a complex morphology (Figs. 1D1 and 1D2, red arrows). These dMBP<sup>+</sup> vesicles varied from 5  $\mu$ m to 25  $\mu$ m in diameter, and while they were predominantly observed in the PVWM and PVSR, some were also found in other DWM regions of AD brains (not shown). The dMBP<sup>+</sup> vesicles were observed in control PVWM (Fig. 1C1, arrow) and PVSR (Fig. 1C2, arrows) as well. The numbers of these “degraded myelin vesicles” (Table 1) were similar in AD compared to control PVSR ( $12.7 \pm 4.4$  versus  $5.8 \pm 2.0$ ) and DWM ( $10.1 \pm 3.2$  versus  $5.2 \pm 2.7$ ), but were significantly increased in PVWM of AD compared to controls ( $44.5 \pm 11.0$  versus  $1.7 \pm 1.1$ ,  $P = 0.02$ ).

Since the vesicles did not stain for intact MBP (Fig. 1B2, arrows), we postulated these vesicles contained degraded MBP. Double immunostaining showed that the vesicles contained degraded MBP (dMBP, Fig. 2A2 and 2A3) but not intact MBP (Figs. 2A1 and 2A3). Therefore, we have referred to these structures as “degraded myelin vesicles” throughout this report. These “degraded myelin vesicles” did not stain for MBP (Figs. 2B1 and 2C1, arrows) but appeared to contain a specific axonal marker, neurofilament (NF) in the PVWM (Figs. 2B2 and 2B3) and PVSr (Figs. 2C2 and 2C3). Double labeling revealed that both NF (Figs. 3A1, 3B1, and 3C1) and dMBP (Figs. 3A2, 3B2, and 3C2) were contained in the walls of the same vesicles in the PVWM (Fig. 3A3), DWM (Fig. 3B3) and PVSr (Fig. 3C3).

### Myelin Lipid Accumulation in Vesicles in AD Brains

Myelin lipid accumulation in the brain was identified with an antibody to galactocerebroside (GALC). There were very few GALC stained vesicles in PVWM (Fig. 4D), DWM (Fig. 4E) and PVSr (Fig. 4F) of control brains. In contrast, there were many GALC stained vesicles in PVWM (Fig. 4A), DWM (Fig. 4B) and PVSr (Fig. 4C) of AD brain. Multiple GALC stained vesicles often occurred in the regions below the denuded ependyma (Fig. 4A, black arrow) in PVWM. Double immunostaining showed that GALC (Figs. 5A1 and 5B1) and dMBP (Figs. 5A2 and 5B2) were contained in the walls of the same “degraded myelin vesicles” in PVWM (Fig. 5A3) and PVSr (Fig. 5B3) in AD brain.

### Degraded Myelin Vesicles Stain with PAS and Represent Corpora Amylacea

Since many dMBP stained vesicles had the morphological appearance and distribution of previously described corpora amylacea (CA), we explored whether these vesicles stained for PAS, a CA marker. Double immunostaining showed that most (Figs. 6A1 and 6B1, white arrows) but not all (Figs. 6A1 and 6A3, yellow arrows) degraded MBP<sup>+</sup> vesicles stained for PAS (Figs. 6A2 and 6B2, black/gray arrows), that appeared to be co-localized (Fig. 6B3, gray and white arrows). Note that in some large and intensely-stained dMBP<sup>+</sup> vesicles (Fig. 6B1, gray arrow), PAS staining was weak (Fig. 6B2, gray arrow) but did co-localize with dMBP (Fig. 6B3, gray arrow). Occasional PAS<sup>+</sup> CA (Fig. 6B2, 6B3, orange arrows) did not stain for dMBP (Fig. 6B1, orange arrow). PAS not only stained vesicles, but also stained vessels (Figs. 6B2 and 6B3, blue arrows), which were negative for dMBP (Fig. 6B1).

## Discussion

This study describes vesicles in white matter containing degraded myelin and axonal proteins in normal aging and AD brain. Since most of these “degraded myelin vesicles” stain with PAS, they are likely corpora amylacea (CA) which have been recognized in aging and AD brains for decades. However, this study is the first to show CA are composed of degraded MBP and other white matter constituents. The degraded myelin vesicles were found to be significantly more numerous in periventricular white matter of patients with AD compared to cognitively normal controls.

### Abnormal “Degraded Myelin Vesicles” in White Matter of AD Brains

We refer to the vesicles associated with degraded myelin basic protein, neurofilament and galactocerebroside as “degraded myelin vesicles”. Most “degraded myelin vesicles” appear to be corpora amylacea (CA) since they stained for PAS, a CA marker [17]. The size, morphology and distribution of the degraded myelin vesicles described in this study and the CA described in the literature are almost identical. CA have been reported to be abundant in PVWM and PVSr [18] as noted in this study. The number of CA is increased in AD compared to control [18], a finding confirmed in this study. Although CA have been associated with cellular stress [19, 20], the origin of CA has not been previously elucidated. Our findings suggest that CA are composed of molecules from damaged WM including dMBP, myelin lipids and axonal proteins. Heat shock proteins and ubiquitin reported in CA [20] could be a molecular chaperone/stress protein response to misfolding of MBP and other myelin proteins in CA.

Though neuropathologists noted vacuolated WM in normal aging and AD brain, there has not been an association of CA with myelin break down products. One study examined myelin in aging and AD brain using the same antibody to dMBP used here. However, the study may not have noted the vesicles/CA since it does not report any findings from PVWM [21].

Occasional PAS stained CA did not stain for dMBP; and occasional degraded myelin vesicles did not stain for PAS. Thus, the relationship of the numerous dMPB<sup>+</sup>/PAS<sup>+</sup> vesicles (CA) to occasional dMPB<sup>+</sup>/PAS<sup>-</sup> vesicles and to occasional dMBP<sup>-</sup>/PAS<sup>+</sup> vesicles is not clear from this study. Further examination in the earliest stages of AD may help reveal the sequence of events related to formation of vesicles from degraded myelin and how this relates to the evolution of PAS staining.

### Myelin Loss and Axonal Degeneration in Normal Aging and AD Brains

There is progressive loss of myelin integrity in late myelinating regions such as the frontal lobe beginning in the fourth of decade of life that is part of normal aging [2]. Loss of myelin staining has been demonstrated in aged animals [22, 23] and humans [24]. Age-related myelin breakdown has been visualized by EM in the absence of loss of neurons or damage to axons [25].

In AD, brain structural changes previously reported in white matter include reduced myelin density, oligodendrocyte loss, axonal loss and astrogliosis [26, 27]. White matter abnormalities have sometimes been described in the absence of axonal damage [28]. In addition, axonal swellings have been reported in AD in the absence of amyloid  $\beta$ -peptide and neurofibrillary tangles [29]. Indeed, myelin breakdown occurs at the earliest stages of AD [2, 4, 6] when neuronal loss is not observed and there are no plaques or tangles [30]. As AD progresses and symptoms become worse, myelin breakdown is more severe [2, 3, 5, 26]. These findings have led to suggestions that myelin breakdown directly contributes to AD pathogenesis [1–6]. Our data support myelin loss in normal aged and AD brains and that the myelin loss relates to the appearance of degraded myelin vesicles, a process which is particularly prominent in PVWM of AD brain.

### Perivascular Loss of Myelin

The data also show that myelin loss can occur around vessels, confirming previous studies [31]. In vascular cognitive impairment where perivascular demyelination also occurs, matrix metalloproteinases are associated with blood brain barrier (BBB) disruption [32]. There is increasing evidence for vascular pathology in AD brain including early onset of hypoperfusion in AD seen by imaging studies [33, 34]. Several investigators have proposed that vascular injury to the BBB and cerebral hypoperfusion can cause WM pathology and eventual gray matter pathology and cognitive decline [35, 36]. Our data support a vascular abnormality in AD which could relate to the perivascular loss of MBP and appearance of degraded myelin vesicles/CA in perivascular regions.

### Ependymal Damage in AD Brain

The finding of ependymal damage and degraded myelin vesicles in control aged brain and in AD brain suggests that loss of ependymal integrity and the process of degraded myelin vesicles formation is not unique to AD. Therefore, whatever the mechanisms of damage of ependyma and formation of degraded myelin vesicles in aging brain, this appears to be exacerbated by AD. Degraded myelin vesicles are abundant in the periventricular white matter and the number of degraded myelin vesicles distinctly increase in AD compared to control.

Several studies have shown that ependymal damage occurs in AD brain. AD brain MRI abnormalities correlate with the loss of myelinated axons in the DWM and with the denudation of the ventricular lining [37]. Pathologically, there are thread- and tangle- like elements in the ependyma and in choroid plexus in patients with cortical AD-type lesions [38]. The ependymal cells in AD brain stain for amyloid and tau protein [38, 39]. Our data confirm loss of ependymal cells in AD brain and demonstrate that myelin loss is adjacent to areas of denuded ependyma, suggesting the notion that loss of ependymal integrity is associated with myelin loss [37] and neurodegeneration [40].

Whether there is any causal link between ependymal damage and periventricular white matter loss as well as formation of degraded myelin vesicles remains to be elucidated. Ependymal cells line the ventricles of central nervous system and separate cerebral spinal fluid from the underlying neuronal tissues. Ependymal cells are reported to be involved in host defense [41]. Therefore, ependyma disruption might allow infiltration of myelinotoxins or pathogens into periventricular white matter and produce myelin damage. In the 3xTg AD mouse model, there is development of large lipid droplets within the ependyma and loss of subependymal cells [42]. Loss of ependyma is of interest since it is immediately adjacent to the subventricular zone where adult neurogenesis occurs, and where decreases of adult neurogenesis occur prior to plaque and tangle formation in the same model [42]. Thus, disruption of ependyma integrity in AD patients and aged brains as seen in this study may be “causal” rather than a consequence of periventricular white matter injury.



## Conclusion

Myelin degradation is increased in Alzheimer's disease patients. The degraded myelin is associated with PAS stained vesicles that are prominent in periventricular white matter adjacent to areas of ependymal injury.

## Acknowledgments

This work was supported by NIH P30 AG10129 (CD), R01 AG021028 (CD) and RO1 NS056302 (FRS/CD).

## References

1. Wallin A, Gottfries CG, Karlsson I, Svennerholm L. Decreased myelin lipids in Alzheimer's disease and vascular dementia. *Acta Neurol Scand.* 1989; 80:319–23. [PubMed: 2816288]
2. Bartzokis G, Cummings JL, Sultzer D, Henderson VW, Nuechterlein KH, Mintz J. White matter structural integrity in healthy aging adults and patients with Alzheimer disease: a magnetic resonance imaging study. *Arch Neurol.* 2003; 60:393–8. [PubMed: 12633151]
3. Chia LS, Thompson JE, Moscarello MA. X-ray diffraction evidence for myelin disorder in brain from humans with Alzheimer's disease. *Biochim Biophys Acta.* 1984; 775:308–12. [PubMed: 6466674]
4. de la Monte SM. Quantitation of cerebral atrophy in preclinical and end-stage Alzheimer's disease. *Ann Neurol.* 1989; 25:450–9. [PubMed: 2774485]
5. Englund E, Brun A, Alling C. White matter changes in dementia of Alzheimer's type. Biochemical and neuropathological correlates. *Brain.* 1988; 111 (Pt 6):1425–39. [PubMed: 3208064]
6. Han X, MHD, McKeel DW Jr, Kelley J, Morris JC. Substantial sulfatide deficiency and ceramide elevation in very early Alzheimer's disease: potential role in disease pathogenesis. *J Neurochem.* 2002; 82:809–18. [PubMed: 12358786]
7. Bartzokis G. Age-related myelin breakdown: a developmental model of cognitive decline and Alzheimer's disease. *Neurobiol Aging.* 2004; 25:5–18. author reply 49–62. [PubMed: 14675724]
8. Gottfries CG, Karlsson I, Svennerholm L. Membrane components separate early-onset Alzheimer's disease from senile dementia of the Alzheimer type. *Int Psychogeriatr.* 1996; 8:365–72. [PubMed: 9116173]
9. Alzheimer A, Forstl H, Levy R. On certain peculiar diseases of old age. *Hist Psychiatry.* 1991; 2:71–101. [PubMed: 11622845]
10. Moller HJ, Graeber MB. The case described by Alois Alzheimer in 1911. Historical and conceptual perspectives based on the clinical record and neurohistological sections. *Eur Arch Psychiatry Clin Neurosci.* 1998; 248:111–22. [PubMed: 9728729]
11. Strittmatter WJ, Saunders AM, Schmechel D, Pericak-Vance M, Enghild J, Salvesen GS, et al. Apolipoprotein E: high-avidity binding to beta-amyloid and increased frequency of type 4 allele in late-onset familial Alzheimer disease. *Proc Natl Acad Sci U S A.* 1993; 90:1977–81. [PubMed: 8446617]
12. Corder EH, Saunders AM, Strittmatter WJ, Schmechel DE, Gaskell PC, Small GW, et al. Gene dose of apolipoprotein E type 4 allele and the risk of Alzheimer's disease in late onset families. *Science.* 1993; 261:921–3. [PubMed: 8346443]
13. Sato H, Tomimoto H, Ohtani R, Kitano T, Kondo T, Watanabe M, et al. Astroglial expression of ceramide in Alzheimer's disease brains: a role during neuronal apoptosis. *Neuroscience.* 2005; 130:657–66. [PubMed: 15590150]
14. Mielke MM, Lyketsos CG. Alterations of the sphingolipid pathway in Alzheimer's disease: new biomarkers and treatment targets? *Neuromolecular Med.* 2010; 12:331–40. [PubMed: 20571935]
15. Lee DY, Fletcher E, Martinez O, Ortega M, Zozulya N, Kim J, et al. Regional pattern of white matter microstructural changes in normal aging, MCI, and AD. *Neurology.* 2009; 73:1722–8. [PubMed: 19846830]

16. Braak H, Braak E. Frequency of stages of Alzheimer-related lesions in different age categories. *Neurobiol Aging*. 1997; 18:351–7. [PubMed: 9330961]
17. Alder N. On the nature, origin and distribution of the corpora amylacea of the brain with observations on some new staining reactions. *J Ment Sci*. 1953; 99:689–97. [PubMed: 13109451]
18. Renkawek K, Bosman GJ. Anion exchange proteins are a component of corpora amylacea in Alzheimer disease brain. *Neuroreport*. 1995; 6:929–32. [PubMed: 7612885]
19. Wilhelmus MM, Verhaar R, Bol JG, van Dam AM, Hoozemans JJ, Rozemuller AJ, et al. Novel role of transglutaminase 1 in corpora amylacea formation? *Neurobiol Aging*. 2011; 32:845–56. [PubMed: 19464759]
20. Cisse S, Perry G, Lacoste-Royal G, Cabana T, Gauvreau D. Immunochemical identification of ubiquitin and heat-shock proteins in corpora amylacea from normal aged and Alzheimer's disease brains. *Acta Neuropathol*. 1993; 85:233–40. [PubMed: 7681614]
21. Ihara M, Polvikoski TM, Hall R, Slade JY, Perry RH, Oakley AE, et al. Quantification of myelin loss in frontal lobe white matter in vascular dementia, Alzheimer's disease, and dementia with Lewy bodies. *Acta Neuropathol*. 2010; 119:579–89. [PubMed: 20091409]
22. Peters A, Moss MB, Sethares C. Effects of aging on myelinated nerve fibers in monkey primary visual cortex. *J Comp Neurol*. 2000; 419:364–76. [PubMed: 10723011]
23. Nielsen K, Peters A. The effects of aging on the frequency of nerve fibers in rhesus monkey striate cortex. *Neurobiol Aging*. 2000; 21:621–8. [PubMed: 11016530]
24. Holland CM, Smith EE, Csapo I, Gurol ME, Brylka DA, Killiany RJ, et al. Spatial distribution of white-matter hyperintensities in Alzheimer disease, cerebral amyloid angiopathy, and healthy aging. *Stroke*. 2008; 39:1127–33. [PubMed: 18292383]
25. Peters A. The effects of normal aging on myelinated nerve fibers in monkey central nervous system. *Front Neuroanat*. 2009; 3:11. [PubMed: 19636385]
26. Brun A, Englund E. A white matter disorder in dementia of the Alzheimer type: a pathoanatomical study. *Ann Neurol*. 1986; 19:253–62. [PubMed: 3963770]
27. Roher AE, Weiss N, Kokjohn TA, Kuo YM, Kalback W, Anthony J, et al. Increased A beta peptides and reduced cholesterol and myelin proteins characterize white matter degeneration in Alzheimer's disease. *Biochemistry*. 2002; 41:11080–90. [PubMed: 12220172]
28. Umahara T, Tsuchiya K, Ikeda K, Kanaya K, Iwamoto T, Takasaki M, et al. Demonstration and distribution of tau-positive glial coiled body-like structures in white matter and white matter threads in early onset Alzheimer's disease. *Neuropathology*. 2002; 22:9–12. [PubMed: 12030417]
29. Stokin GB, Lillo C, Falzone TL, Brusch RG, Rockenstein E, Mount SL, et al. Axonopathy and transport deficits early in the pathogenesis of Alzheimer's disease. *Science*. 2005; 307:1282–8. [PubMed: 15731448]
30. Price JL, Ko AI, Wade MJ, Tsou SK, McKeel DW, Morris JC. Neuron number in the entorhinal cortex and CA1 in preclinical Alzheimer disease. *Arch Neurol*. 2001; 58:1395–402. [PubMed: 11559310]
31. Kirkpatrick JB, Hayman LA. White-matter lesions in MR imaging of clinically healthy brains of elderly subjects: possible pathologic basis. *Radiology*. 1987; 162:509–11. [PubMed: 3797666]
32. Candelario-Jalil E, Thompson J, Taheri S, Grossetete M, Adair JC, Edmonds E, et al. Matrix metalloproteinases are associated with increased blood-brain barrier opening in vascular cognitive impairment. *Stroke*. 2011; 42:1345–50. [PubMed: 21454822]
33. Farkas E, Luiten PG. Cerebral microvascular pathology in aging and Alzheimer's disease. *Prog Neurobiol*. 2001; 64:575–611. [PubMed: 11311463]
34. Kalaria RN. Cerebral vessels in ageing and Alzheimer's disease. *Pharmacol Ther*. 1996; 72:193–214. [PubMed: 9364575]
35. Zlokovic BV. Neurovascular pathways to neurodegeneration in Alzheimer's disease and other disorders. *Nat Rev Neurosci*. 2011; 12:723–38. [PubMed: 22048062]
36. Horsburgh K, Reimer MM, Holland P, Chen G, Scullion G, Fowler JH. Axon-glia disruption: the link between vascular disease and Alzheimer's disease? *Biochem Soc Trans*. 2011; 39:881–5. [PubMed: 21787317]

37. Scheltens P, Barkhof F, Leys D, Wolters EC, Ravid R, Kamphorst W. Histopathologic correlates of white matter changes on MRI in Alzheimer's disease and normal aging. *Neurology*. 1995; 45:883–8. [PubMed: 7746401]
38. Miklossy J, Kraftsik R, Pillevuit O, Lepori D, Genton C, Bosman FT. Curly fiber and tangle-like inclusions in the ependyma and choroid plexus--a pathogenetic relationship with the cortical Alzheimer-type changes? *J Neuropathol Exp Neurol*. 1998; 57:1202–12. [PubMed: 9862643]
39. Barnum SR. Complement biosynthesis in the central nervous system. *Crit Rev Oral Biol Med*. 1995; 6:132–46. [PubMed: 7548620]
40. Radojicic M, Nistor G, Keirstead HS. Ascending central canal dilation and progressive ependymal disruption in a contusion model of rodent chronic spinal cord injury. *BMC neurology*. 2007; 7:30. [PubMed: 17822568]
41. Hoarau JJ, Krejbich-Trotot P, Jaffar-Bandjee MC, Das T, Thon-Hon GV, Kumar S, et al. Activation and control of CNS innate immune responses in health and diseases: a balancing act finely tuned by neuroimmune regulators (NIReg). *CNS & neurological disorders drug targets*. 2011; 10:25–43. [PubMed: 21143144]
42. Hamilton LK, Aumont A, Julien C, Vadnais A, Calon F, Fernandes KJ. Widespread deficits in adult neurogenesis precede plaque and tangle formation in the 3xTg mouse model of Alzheimer's disease. *The European journal of neuroscience*. 2010; 32:905–20. [PubMed: 20726889]

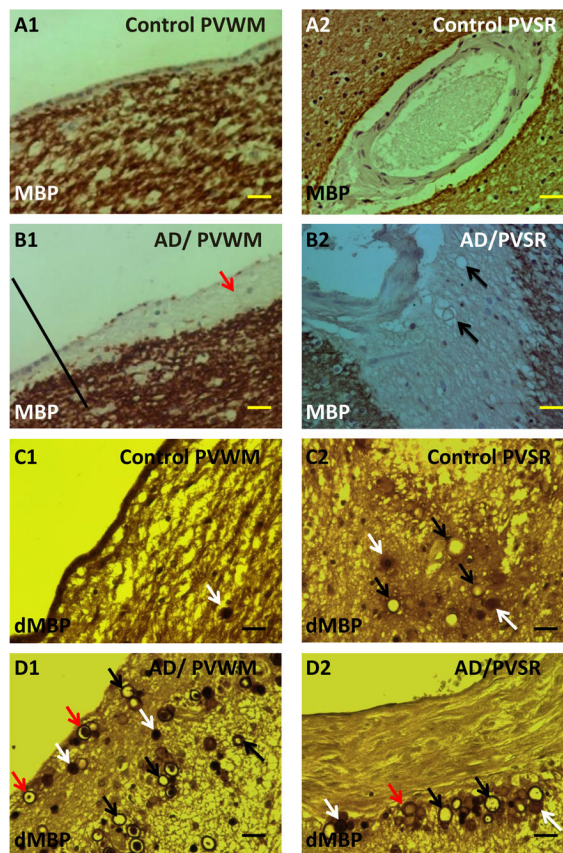


**Fig. 1. Myelin loss and degraded myelin vesicles in the white matter of Alzheimer's disease (AD) brains**

In controls, intact MBP staining was observed in the PVWM (Periventricular White Matter) (A1) and around the white matter of PVSR (Perivascular Region of white matter) (A2). In PVWM of AD brains, there was loss of ependymal cells adjacent to the ventricle (B1). There was marked decrease of staining for intact MBP in the PVWM adjacent to the denuded ependyma (B1, red arrow). Note more intact ependymal cells to the left of the black line along with intact MBP staining being closer to the ependymal layer (B1). There was decreased MBP staining in the PVSR of AD brains (B2) and vesicles in these regions did not stain for intact MBP (B2, arrows).

An antibody specific for degraded MBP (dMBP) was used to detect degraded myelin in AD and control brains. In areas of decreased overall MBP staining, dMBP immunostaining was detected mainly in different types of vesicles: solid (D1 and D2, white arrows), clear (D1 and D2, black arrows), and a complex morphology (D1 and D2, red arrows). In control, few dMBP<sup>+</sup> vesicles were detected (C1 and C2, arrows) in PVWM. These “degraded myelin vesicles” varied in sizes from 5  $\mu$ m to 25  $\mu$ m. Brown = positive staining, MBP = intact myelin basic protein, dMBP = degraded MBP, AD= Alzheimer's disease. Bars = 25 $\mu$ m.

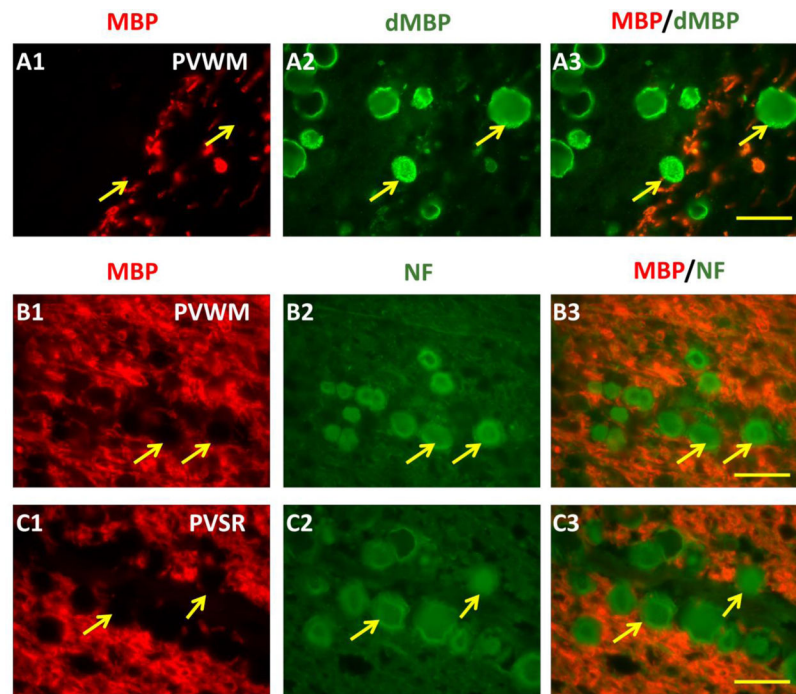


**Fig. 2. Identification of “degraded myelin vesicles” in regions of myelin loss in AD brains**  
 Double labeling showed that in the area absent of intact-MBP (A1, arrows), degraded MBP<sup>+</sup> vesicles (A2 and A3, arrows) were observed. In addition, in the area absent of intact-MBP (B1 and C1, arrows), a specific axonal marker, NF was stained in the vesicles (B2 and B3, PVWM; C2 and C3, PVSR) were observed. MBP = intact myelin basic protein, dMBP = degraded MBP, NF = neurofilament, PVWM = periventricular white matter, PVSR = perivascular region of white matter. Bars = 25 $\mu$ m.

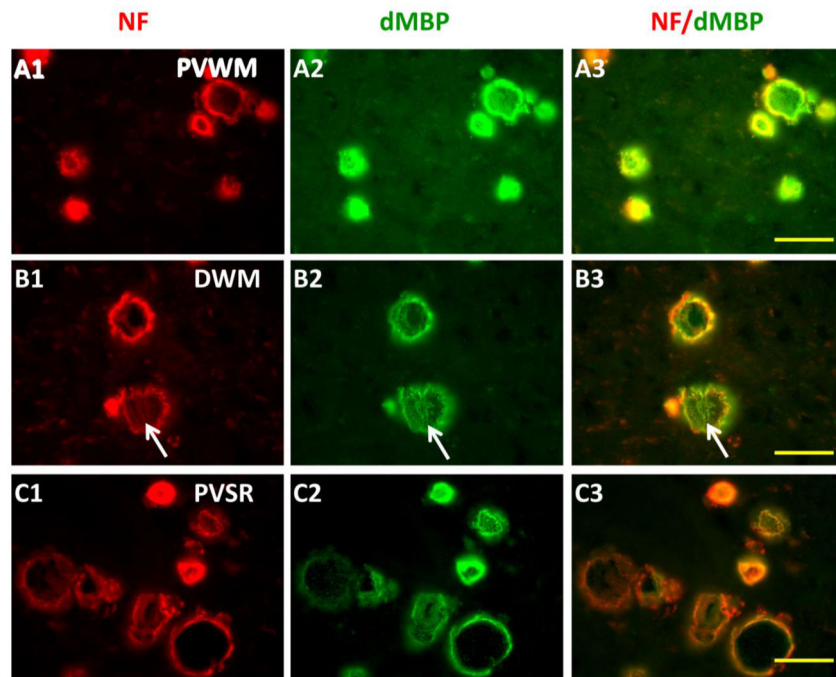


**Fig 3. Co-localization of NF and dMBP in the vesicles of AD brains**

Double labeling showed that NF (A1, B1 and C1) and dMBP (A2, B2 and C2) were co-localized in the same vesicles (A3, B3 and C3). dMBP = degraded MBP, NF = neurofilament, PVWM = periventricular white matter, DWM = deep white matter, PVSR = perivascular region of white matter. Bars = 25 $\mu$ m.

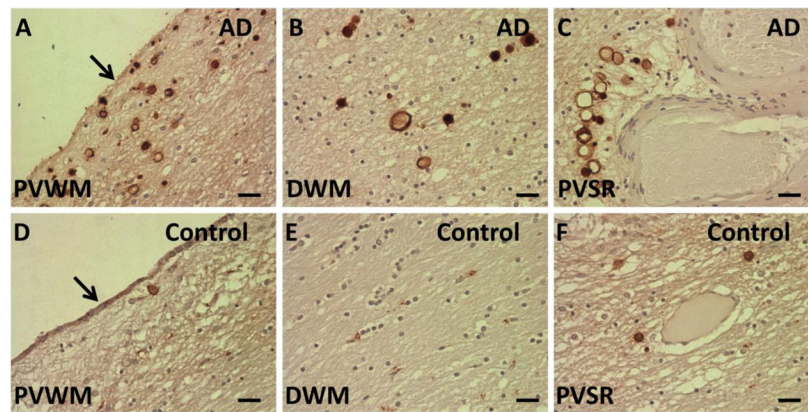


**Fig 4. Localization of myelin lipid in the vesicles in AD brains**

Galactocerebroside (GALC), a myelin lipid, was localized in the vesicles of PVWM (A), vesicles in DWM (B) and vesicles in PVSR (C) in AD brains. In age matched control brains there were fewer GALC<sup>+</sup> vesicles in PVWM (D), DWM (E) and PVSR (F). Note that the GALC<sup>+</sup> ependymal cells were lost in the AD brain (A) but GALC<sup>+</sup> ependymal cells were present in control (D). Brown = positive staining, AD = Alzheimer's disease, PVWM = periventricular white matter, DWM = deep white matter, PVSR = perivascular region of white matter. Bars = 25 $\mu$ m.

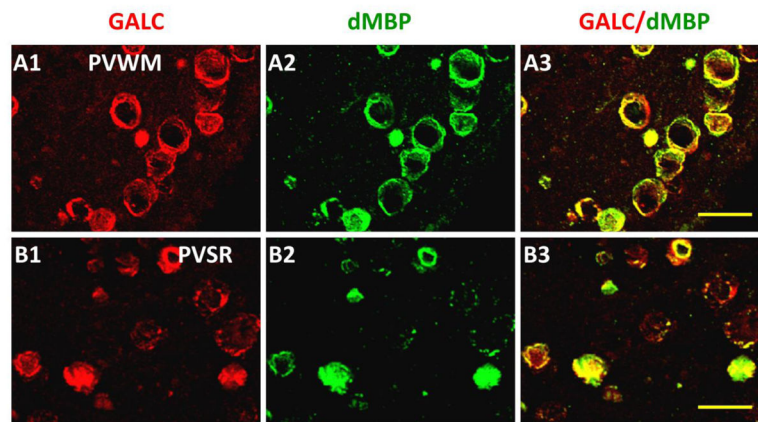


**Fig 5. Localization of myelin lipid in the degraded myelin vesicles in AD brains**  
Galactocerebroside (GALC) (A1 and B1), a myelin lipid, was localized in the dMBP<sup>+</sup> vesicles (A2, A3, B2 and B3) of PVWM (A1, A2,A3) and PVSr (B1, B2, B3) in AD brains. PVWM = periventricular white matter. PVSr = perivascular region of white matter, Bars = 25 $\mu$ m.



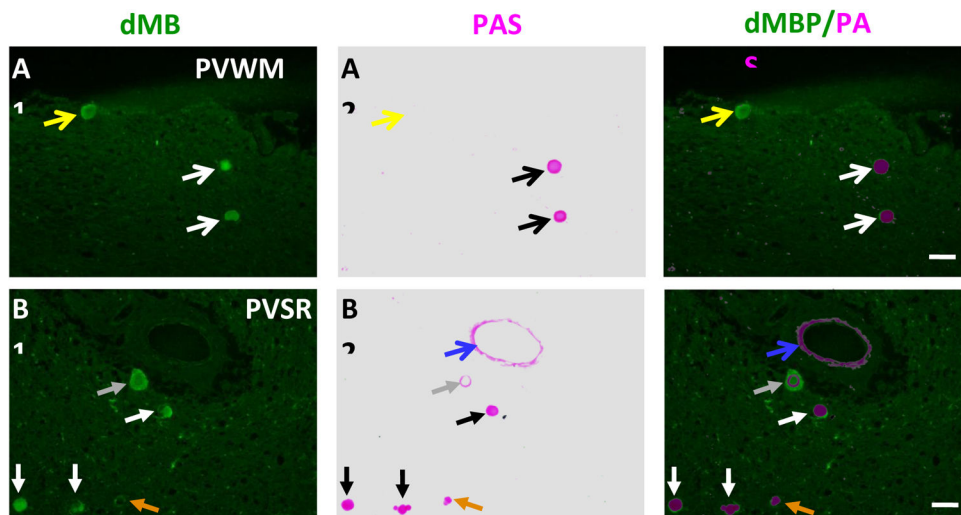


**Fig 6. Double staining of dMBP and PAS in AD brains**

dMBP<sup>+</sup> vesicles (A1, B1, white arrows) often stained for PAS, a corpora amylacea marker (A2, B2, black arrows) that appeared to be co-localized (A3, B3). Occasional dMBP stained vesicles (A1, yellow arrow) did not stain for PAS (A2, A3 yellow arrows). Note that in some large and intensely-stained dMBP<sup>+</sup> vesicles (B1, gray arrow), PAS staining was weak (B2, gray arrow) but did co-localize with dMBP (B3, gray arrow). Occasional PAS stained vesicles (B2, B3, orange arrows) did not stain for dMBP (B1, orange arrow). PAS not only stained vesicles, but also stained vessels (B2 and B3, blue arrows), which were negative for dMBP (B1). PVWM = periventricular white matter; PVSr = perivascular regions of white matter; dMBP, degraded myelin basic protein; PAS, periodic acid-Schiff. Bars = 25 $\mu$ m.

**Table 1**

Demographic data and pathology ratings in AD patients and controls

	Controls (n=6)	AD (n=13)
Age (years $\pm$ standard error)	79.8 $\pm$ 3.2	83.7 $\pm$ 1.5
Gender Male: n (%)	3 (50.0)	6 (46.2)
Braak stage: median	2 (IQR 2, 2)	6 (IQR 4, 6) ***
Previous stroke: n (%)	2 (33.3)	3 (23.1)
Number of vesicles in PVWM	1.7 $\pm$ 1.1	44.5 $\pm$ 11.0 *
Number of vesicles in DWM	5.2 $\pm$ 2.7	10.1 $\pm$ 3.2
Number of vesicles in PVSR	5.8 $\pm$ 2.0	12.7 $\pm$ 4.4
Ependyma loss, none: n (%)	2 (33.3)	2 (15.4)
Ependyma loss, mild: n (%)	1 (16.7)	0 (0)
Ependyma loss, moderate: n (%)	2 (33.3)	0 (0)
Ependyma loss, severe: n (%)	1 (16.7)	11 (84.6) **

Number of vesicles expressed as mean  $\pm$  standard error/20X field area (about 0.8 mm<sup>2</sup>). Differences between groups analyzed using a Student t-test (continuous), Wilcoxon-Mann Whitney test (ordinal) and Fisher Exact test (categorical). AD, Alzheimer's disease; DWM, deep white matter; IQR, interquartile range; PVWM, periventricular white matter; PVSR, periventricular space region of white matter; mild: ependyma loss  $\leq$  25%; moderate: 25% > ependyma loss  $\leq$  50%; severe: ependyma loss > 50%;

\* P < 0.05 for AD vs controls;

\*\* P < 0.01 for AD vs controls;

\*\*\* P < 0.001 for AD vs controls.